



# **The response of optical emission on heating of the ionosphere by powerful radio wave**

J. Legostaeva, A. Shindin, and S. Grach  
Lobachevsky University, Nizhny  
Novgorod, Russia 603105  
julilegostaeva@gmail.com

# Introduction

We model the effect of suppression of the background airglow during the heating as well as its recovery and “afterglow” after the heating switching off. Results obtained allow to estimate the increase of electron temperature and rates of some photo-chemical reactions in the heated ionosphere.

Optical emission of atomic oxygen (state  $O^1D$ , 630 nm, red line excitation threshold 1.96 eV) of the HF-pumped ionosphere exhibits two opposite effects:

1) the enhancement of the emission intensity (artificial optical emission or artificial aurora) due to increasing collisional excitation of  $O^1D$  caused by electron acceleration by parametrically excited plasma waves

2) the suppression of the background emission due to slowing down dissociative recombination of electrons ( $e$ ) and molecular oxygen ions ( $O_2^+$ ) with increasing electron temperature  $a(T_e) \propto T_e^{-1/2}$ ,  $a$  is the recombination coefficient.

The purpose of the work is numerical simulations of the second effect, namely, the dynamics of the ionosphere red line emission caused by powerful radio wave switching on and off, and comparing simulation results with experimental data obtained at the SURA heating facility

# Experimental data

Experimental results were obtained at the SURA facility on September 14, 2012. SURA facility radiated vertically at the frequency 5.33 MHz with a schedule 150 s "on", 270 s "off". The effective radiated power was  $P_{\text{ef}} \sim 200$  MW. The night-sky images presented were obtained with CCD camera S1C/079-FP(FU) with 20.6° field of view equipped with interference light filter for the wavelength  $\lambda = 630$  nm (having a passband  $\Delta\lambda_{0.5} = 10$  nm and a transmittance of 65%) The exposure time was 15 s.

# Experimental data. HF-induced enhancement

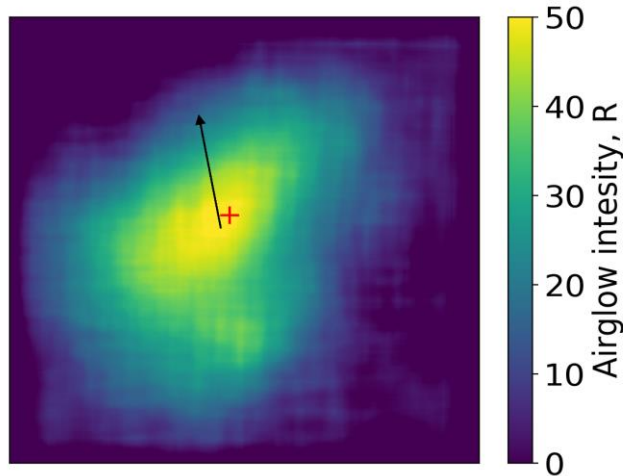


Figure 1. Night sky image in the atomic oxygen red line (630 nm) with HF pump induced emission enhancement. SURA Facility, 14.09.2012, 18:09 UTC (22:09 local summer time). The arrow shows the direction to geographical North.

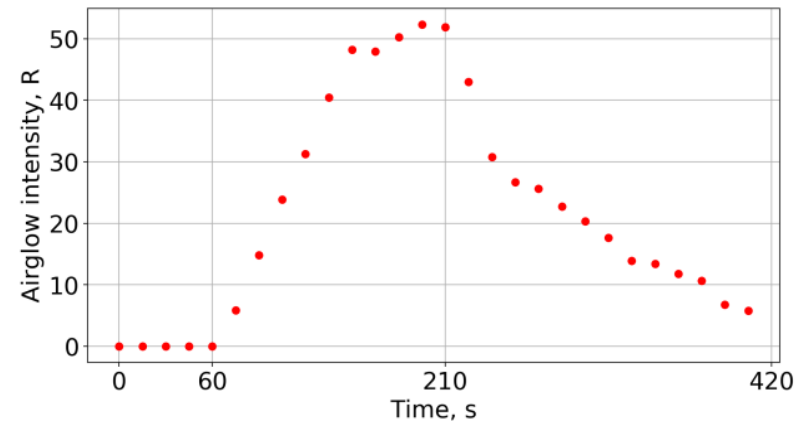


Figure 2. The 630 nm airglow intensity dynamics measured on the ground during 18:06 – 18:13 UTS 14.09.2012.  $t = 60$  s corresponds to the pump wave switching on,  $t = 210$  s to the pump wave switching off.

The maximum brightness in the image achieves 50 R (red cross). The brightness dynamics is shown at the point with maximum brightness across the camera field of view shown by red cross in the Figure 1. It is seen that in  $\sim 25$  s after heating switch off the decay of the airglow brightness slows down. In some sessions even an increase in brightness is observed in this time, we call this “afterglow”.

# Experimental data. Background suppression

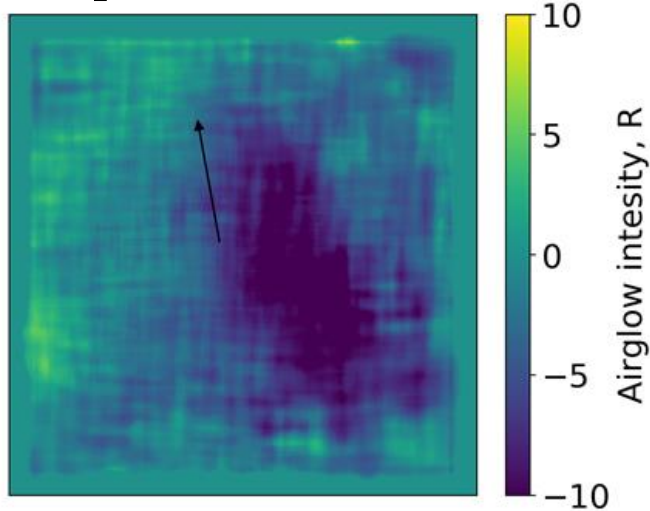


Figure 3. The same as in Fig. 1 but for 18:13 UTS (next session of the heating 18:12 – 18:19 14.09.2012).

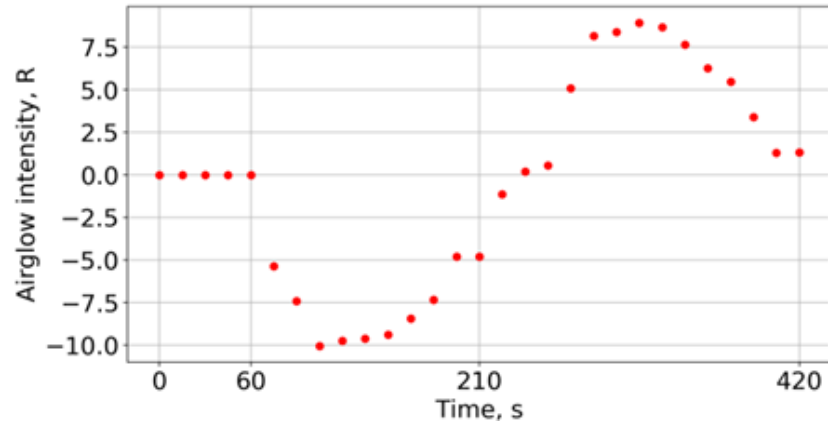


Figure 4. The 630 nm brightness dynamics measured on the ground during 18:12 – 18:19 UTS

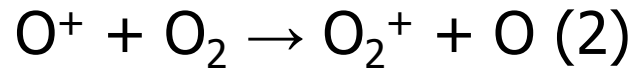
In this session the suppression reaches 10 R already in  $\sim 50$  s after pump wave switching on. Then the emission intensity starts to recover. The recovery continues after heating switching off till  $t=310$ - $320$  s, and then slowly decays. During  $240$  s  $< t < 420$  s the airglow brightness exceeds the stationary background level without heating (afterglow).

# Theoretical model

The red line airglow measured in the experiment is determined as the integral over the entire range of heights where excited atoms  $O^1D$  exist:

$$B = A_{6300} \int [O^1D] dz \quad (1),$$

where  $A_{6300} = 7,1 \cdot 10^{-3}$  is the Einstein coefficient,  $[O^1D]$  is the concentration of excited atoms. Under natural conditions (in the absence of the HF heating), the maximum of  $[O^1D] \sim 1200 \text{ cm}^{-3}$  is reached at altitudes 230-250 km. At these altitudes, excited atoms in the  $O^1D$  state appear as a result of a sequence of charge exchange reaction



and dissociative recombination of electrons with molecular oxygen ions



# Theoretical model

The system of differential equations describing the dynamics of  $[O_2^+]$  and  $[O^1D]$  under reaction of dissociative recombination (3) and reaction of charge exchange (2) with account of the electron heating, takes the form:

$$\frac{d[O_2^+]}{dt} = k_1[O^+][O_2] - \alpha[O_2^+]N_e \quad (4)$$

$$\frac{d[O^1D]}{dt} = \eta\alpha[O_2^+]N_e - \frac{1}{\tau_{\text{eff}}}[O^1D], \quad (5)$$

$$\frac{\partial T_e}{\partial t} - D_T \frac{\partial^2 T_e}{\partial z^2} + \delta\nu_e(T_e - T_0) = Q_T. \quad (6)$$

$\tau_{\text{eff}}$  is the effective lifetime of the atom in the state  $O^1D$ .

$\tau_{\text{eff}}$  is different from the radiation lifetime  $\tau_r = 107$  s. In calculating  $\tau_{\text{eff}}$ , the decrease in the concentration of the excited atoms in the  $O^1D$  state as a result of deactivation in collisions with nitrogen and oxygen molecules  $N_2$ ,  $O_2$  are taken into account. In calculations we take  $\tau_{\text{eff}} = 35$  s.

# Theoretical model

Here  $k_1 = 2 \cdot 10^{-11} \frac{\text{cm}^3}{\text{s}}$  is the rate coefficient of the charge exchange reaction (2),  $\alpha$  is the coefficient of dissociative recombination,  $\alpha(T_e) = \alpha_0 \sqrt{\frac{T_0}{T_e}}$ ,  $\alpha_0 = 1,9 \cdot 10^{-7} \sqrt{\frac{300}{T_0}}$ ,  $T_0 = 1000 \text{ }^\circ\text{K}$  is electron temperature at the powerful wave turning on (beginning of heating),  $N_e$  is the electron density,  $\eta = 1.1$  is the probability coefficient.



# Theoretical model

Eq. (6) is the electron thermal conductivity equation with the source  $Q_T(z, t)$  situated near  $z_0$ , the upper hybrid resonance height of powerful radio wave, related to the electron heating by the pump (electromagnetic) wave and parametrically excited plasma waves.

$$Q_T(z, t) = Q_T(z) = \frac{2E_0^2}{3N_e} \frac{v_e}{4\pi} \epsilon \left[ h\left(z - \left[z_0 - \frac{\Delta z}{2}\right]\right) - h\left(z - \left[z_0 + \frac{\Delta z}{2}\right]\right) \right] [h(t - t_{\text{on}}) - h(t - t_{\text{off}})].$$

The initial condition for Eq. (6) is  $T_e(z, t = 0) = T_0$ .

$h(z)$  is the Heaviside function,  $z$  is the height,  $z_0$  the upper hybrid resonance height, is the height of the center of the heating source,  $\Delta z = 1$  km is the characteristic width of the heating source,  $t_{\text{on}}$  and  $t_{\text{off}}$  are the times of turning on and off the powerful wave, respectively,  $D_T = l_e v_e^2$ ,  $l_e = 600$  m is the mean free path,  $\delta = 10^{-4}$  is the fraction of energy lost by the electron during collision with heavy particle,  $m_e$  is the mass of the electron and  $\nu_e = 300$  s<sup>-1</sup> is the electron collision frequency,  $E_0^2$  is the intensity of the pump wave electric field. For calculations, we use for  $E_0$  the formula  $E_0(z)[\text{V/m}] = 9.5 \frac{\sqrt{W_0[\text{kW}]}}{z(\text{m})}$ , where  $W_0 = 175$  kW is the power of the transmitter pumping the ionosphere.  $\epsilon \gg 1$  is coefficient enlarging the source due to inclusion of plasma waves in heating process.

# Theoretical model

Based on the solution of equations (4) - (6), the height distribution of concentrations  $[O_2]$  and  $[O]$ , taken from the empirical model of the atmosphere NRLMSISE-00, and the electron concentration profile  $N_e$ , taken from the International Reference Ionosphere model (IRI) and modified taking into account the conditions of the experiment, a behavior of the concentration  $[O^1D]$  and the brightness of the optical glow in the ionospheric experiments performed at the SURA facility was modeled.

# Results of modelling

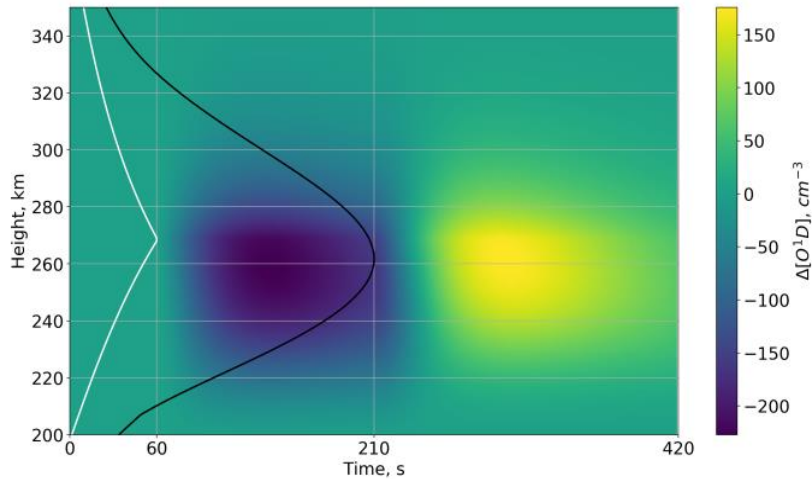


Figure 5. Simulations of heating-induced excited oxygen  $O^1D$  concentration vs. time for the session 18:07 – 18:13 UTS. Black and white lines illustrate height distribution of  $[O^1D]$  without heating and the electron temperature  $T_e$  height distribution before heating switching off. The maximum of  $[O^1D]$  is  $1200 \text{ cm}^{-3}$ ,  $T_e$  maximum is 800 K.

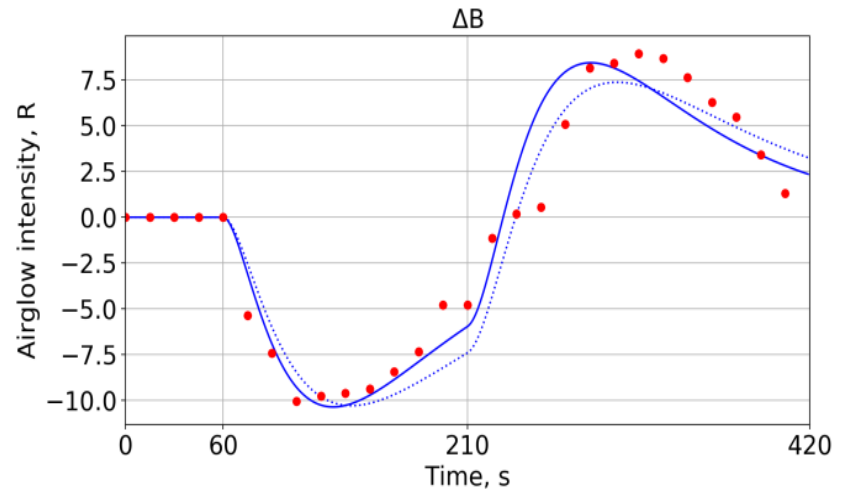


Figure 6. Temporal evolution of 630 nm brightness for the session 18:07 – 18:13 UTS.  $t = 60 \text{ s}$  corresponds to the pump wave switching on,  $t = 210 \text{ s}$  to the pump wave switching off. Red dots present the experimental data taken from Fig.4, dashed line corresponds to the modeling with parameters shown in the Section 3 with  $\epsilon = 15$ . For solid line the following parameters were taken:  $\epsilon = 20$ ,  $\alpha(T_e) = 1.5\alpha_0(T_0/T_e)^{1/2}$ .

# Results of modelling

Figure 5 displays the distribution of  $[O^1D]$  for the heating source position  $z_0=270$  km after subtraction of the background. Figure 6 exhibits the emission brightness dynamics on the ground for two different sets of the of simulation parameters: the same as in Fig. 5 (dashed line) and (solid line) slightly varied for better coincidence with experimental data (red dots taken from Fig. 4). From Figs. 5, 6 it is seen that temporal behavior of the measured emission brightness is qualitatively similar to one obtained from simulations.

# Discussion

The suppression of the emission intensity is determined by a decrease in the coefficient of dissociative recombination  $\alpha$  with increasing electron temperature, a decrease in  $[O^1D]$  in accordance with equation (4), and, consequently, the brightness of optical emission  $B$ . When the pump wave is turned off, the electrons cool down,  $T_e$  decreases,  $\alpha$  and, therefore,  $[O^1D]$  increase, which leads to a temporary increase in brightness (afterglow). The characteristic times of brightness variations during simulation is determined by the reaction coefficients and, as we see, are close to the experimentally observed ones. With some, perhaps arbitrary, variations of the simulation parameters, it is possible practically to combine the theoretical curve with the experimental points. Variations of parameters are given in the captions to Figures 5, 6.

Notice that for the long heating ( $t > 150$  s in our case) the stationary ( $\partial/\partial t=0$ ) brightness value  $B$  equal to the initial one ( $B=0$  in the Fig. 6) should be achieved. The same brightness should be attained after the heating switching off and temporary brightness increase (afterglow).

# Discussion

Thus, modeling the effect of electron heating on the behavior of the glow in the 630 nm line may be useful for estimating a number of ionosphere parameters. In particular, there are a concentration of excited oxygen atoms and its variations during and after heating, the height of the glow source in the red line, the magnitude of the electron temperature increase under heating, the reaction coefficients responsible for the brightness dynamics.

At the same time, it remains unclear why in some successive heating sessions very close in time, an abrupt change in the observed effect can happen: a brightness growth in a compact spot with its suppression in a sufficiently wide region is replaced by heating sessions when the electron acceleration does not exist or is very weak, and the suppression of the airglow prevails and is observed.

**Thank you for attention!**